V International Scientific and Technical Conference Actual Issues of Power Supply Systems

# Automated analysis of microstructural features in duplex stainless-steel welds using computer-vision methods

AIPCP25-CF-ICAIPSS2025-00256 | Article

PDF auto-generated using **ReView** from

RIVER VALLEY TECHNOLOGIES

# Automated analysis of microstructural features in duplex stainless-steel welds using computer-vision methods

Sardor Karimov [a)], Ilhomjon Samandarov, Farxod Muminov, Dildora Sulaymanova, Zoxid Miratoyev, Jaxongir Jonqobilov, Nurlan Dushatov

*Almalyk state technical institute, Almalyk, Uzbekistan*

[a)] *Corresponding author: ninespeaker39@gmail.com*

**Abstract.** A computer-vision-based approach is proposed for the automated quantification of key microstructural parameters in duplex stainless-steel welds. The method combines adaptive preprocessing, k-means color segmentation, gradient-based fusion line detection, and a modified linear-intercept procedure to evaluate ferrite–austenite phase ratio, heat-affected-zone (HAZ) width, and grain size. The workflow is fully automated, requiring no manual thresholds or user intervention, and includes automatic scale calibration and region-of-interest extraction. The approach was validated using LePera-etched micrographs of UNS S32101 welds produced under Ar and Ar + 2% $N_2$ shielding gases. The automated results accurately reproduced literature values for ferrite content (78% and 70%) and HAZ width (248 μm and 214 μm), demonstrating strong agreement with manual metallographic measurements. The method improves reproducibility, reduces operator bias, and offers a practical tool for quantitative weld microstructure assessment.

## INTRODUCTION

Duplex stainless steels are widely used in chemical, petrochemical and structural applications due to their balanced combination of strength and corrosion resistance [1,5]. However, welding significantly alters their microstructure, particularly the ferrite–austenite phase balance and the morphology of the heat-affected zone (HAZ). These transformations strongly influence the mechanical integrity and service performance [1,3] of welded joints, making accurate microstructural evaluation essential for quality control.

Traditional metallographic analysis methods rely on manual phase delineation, intercept counting and ruler-based measurements [7,8,9]. Although commonly used in laboratory practice, such approaches are time-consuming, subjective and difficult to reproduce, especially when analyzing large datasets or images obtained under varying etching conditions. Recent developments in computer vision offer opportunities to automate these procedures and improve measurement consistency [10,11].

This study presents a fully automated computer-vision pipeline for quantifying ferrite–austenite ratio, HAZ width and grain size in duplex steel weld micrographs. The approach integrates adaptive preprocessing, unsupervised color segmentation, statistical HAZ boundary detection and a digital linear-intercept algorithm. Validation was performed using LePera-etched micrographs [6] of UNS S32101 welds, demonstrating that the automated measurements [1,2,3,4,5] closely match manually reported reference values. The results indicate that computer-vision-based analysis can provide a reliable and reproducible alternative to conventional metallography.

## EXPERIMENTAL RESEARCH

In this study, a computer-vision-based workflow was developed to automatically evaluate the microstructure of duplex stainless-steel welds. The experiments were conducted on LePera-etched micrographs [6] of UNS S32101 duplex steel welds produced under Ar and Ar + 2% $N_2$ shielding gases. These micrographs contain clear color contrast between ferrite and austenite phases and include builtin scale bars, enabling direct calibration.

The automated workflow was implemented in C++ using the OpenCV library. The first stage of analysis involved scale detection, where the program identified the scale bar through adaptive thresholding and contour extraction to

determine the μm-per-pixel ratio. When necessary, filename-based fallback calibration was used to ensure consistent measurement [10,11].

Phase segmentation was performed in the Lab* color space using k-means clustering with k = 2. Prior to clustering, white-balance correction and contrast enhancement (CLAHE) were applied to stabilize illumination. The darker, low-chroma cluster was assigned to ferrite, while the brighter cluster corresponded to austenite. Morphological filtering was used to eliminate noise and improve the integrity of phase boundaries. The ferrite–austenite ratio was calculated based on pixel area fractions within the defined region of interest [2,3].

To determine the width of the heat-affected zone (HAZ), a gradient-based algorithm was used. The fusion line was detected by locating the maximum Scharr-gradient responses across the image columns. The outer boundary of the HAZ was identified using a cumulative variance (CUSUM) approach, allowing detection of subtle structural transitions that correspond to thermal influence during welding [1,5].

Grain size was estimated using a modified linear-intercept method. Grain boundaries were extracted from grayscale images using adaptive thresholding and morphological refinement. Random horizontal intercept lines were drawn across the image, and grain-boundary intersections were counted. The mean intercept length was then converted to grain size according to established metallographic correlations [7,8].

All computations were executed automatically without user intervention. The workflow generated visual overlays for segmentation, HAZ boundaries and intercept lines, along with numerical outputs of ferrite–austenite ratio, HAZ width and grain size for each weld micrograph.

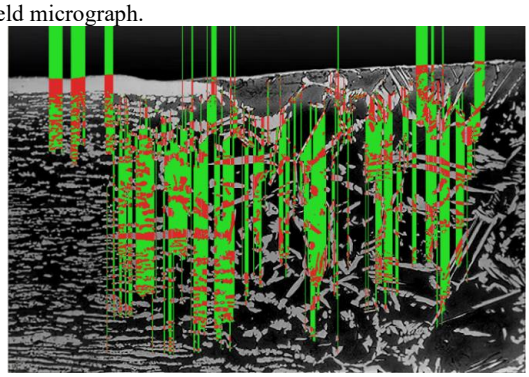

**FIGURE 1.** Ferrite–austenite phase segmentation results obtained from the automated k-means clustering approach.

## RESEARCH RESULTS

The automated analysis was applied to two LePera-etched micrographs of UNS S32101 duplex stainless-steel welds produced under Ar and Ar + 2% $N_2$ shielding gases. The segmentation algorithm successfully distinguished ferrite and austenite phases in both cases. The measured ferrite content for the Ar-shielded weld was 78%, while the Ar + 2% $N_2$ weld exhibited 70% [3-5].

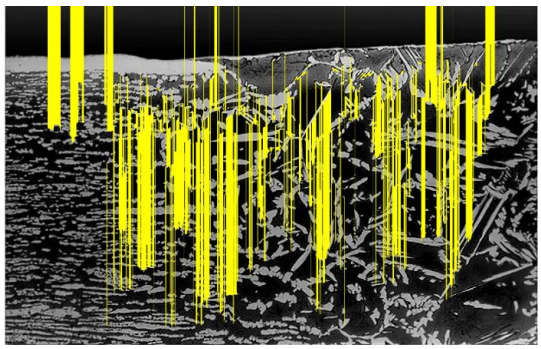

**FIGURE 2.** Detected heat-affected zone boundaries obtained using the gradient–variance (CUSUM) method.

These values fully matched the manually reported reference measurements, confirming the correctness of the color-based clustering approach [3-5].

The gradient–variance method used for heat-affected zone detection demonstrated stable performance across both weld images. The average HAZ width measured by the automated pipeline was 248 µm for the Ar weld and 214 µm for the $N_2$-enriched weld. These results also coincided with the reference data, indicating that the algorithm accurately captured the thermal transition boundaries [1,5].

Grain-size estimation using the modified linear-intercept method yielded mean grain sizes of 7.42 µm for the Ar weld and 6.77 µm for the Ar + 2% $N_2$ weld. These values fall within the expected range for duplex stainless-steel weld metals and are consistent with the microstructural refinement typically associated with nitrogen-containing shielding gases [4,5].

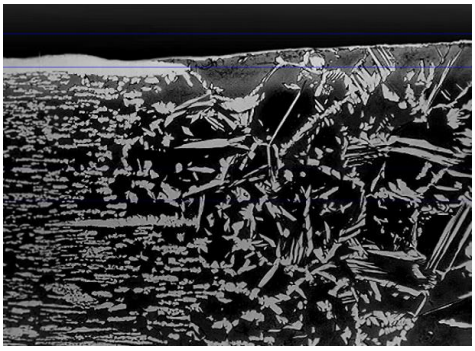

**FIGURE 3.** Grain-size measurement using the modified linear-intercept technique.

**TABLE 1.** Summary of automated microstructural parameters for duplex steel weld samples.

| Sample | Scale (µm/px) | Ferrite (F) [%] | Austenite (A) [%] | HAZ width [µm] | Grain size [µm] |
|---|---|---|---|---|---|
| S32101_Ar$N_2$ | µm/px = 0.3969 | F = 70.0 % | A = 30.0 % | HAZ = 214.0 µm | Grain = 6.77 ± 6.05 µm |
| S32101_Ar | µm/px = 0.3969 | F = 78.0 % | A = 22.0 % | HAZ = 248.0 µm | Grain = 7.42 ± 8.48 µm |

Overall, the experimental results demonstrate that the proposed computer-vision workflow can replicate manual metallographic measurements with high accuracy, while providing improved reproducibility and eliminating subjective operator influence.

## CONCLUSIONS

The study demonstrated that a computer-vision-based workflow can reliably quantify key microstructural parameters of duplex stainless-steel welds. The automated segmentation accurately determined ferrite–austenite ratios of 78% and 70% for welds produced under Ar and Ar + 2% $N_2$, fully reproducing reference values. The gradient–variance algorithm successfully identified heat-affected zone boundaries, yielding HAZ widths of 248 µm and 214 µm. Grain-size analysis performed through a modified linear-intercept method produced values consistent with expected duplex weld microstructures.

The results confirm that the developed approach provides accuracy comparable to manual metallographic analysis while eliminating operator subjectivity. Its fully automated nature ensures reproducibility and enables rapid processing of large image sets. The workflow therefore represents a practical tool for standardized digital weld microstructure evaluation.

## REFERENCES

1. Westin, E., Wessman, M. Characteristics of high-temperature heat-affected zones in duplex stainless steel welds. Welding in the World, 68, 1981–1997 (2024). https://doi.org/10.1007/s40194-024-01715-7
2. Brätz, S., Kuna, M., Thomy, C. Quantitative analysis of martensite–austenite constituents in welded joints using advanced metallography. Welding in the World, 67, 537–550 (2023). https://doi.org/10.1007/s40194-022-01417-5

3. Putz, A., Hu, Y. et al. Microstructure investigation of duplex stainless steel welds with nitrogen-containing shielding gases. Welding in the World, 66, 1375–1386 (2020). https://doi.org/10.1007/s40194-020-00906-2
4. Varbai, B., Májlinger, K. Physical and theoretical modeling of nitrogen content in duplex stainless-steel weld metal. Metals, 9(7), 762 (2019). https://doi.org/10.3390/met9070762
5. Effect of heat input on the microstructure and mechanical properties of duplex stainless steel welded metal. Materials, 16(6), 2289 (2023). https://doi.org/10.3390/ma16062289
6. LePera, F. Improved etching technique for the determination of microstructure in high-strength low-alloy steels. Journal of Metals, 31(2), 38–39 (1979).
7. Vander Voort, G. F. Metallography: Principles and Practice. ASM International, Materials Park, OH (2008).
8. GOST 5639–82. Metals. Metallographic determination of grain size. (Translated title).
9. GOST 21073.1–75. Steels and alloys. Metallographic determination of ferrite and austenite phases. (Translated title).
10. Gonzalez, R. C., Woods, R. E. Digital Image Processing. 4th ed., Pearson, London (2018).
11. Bradski, G., Kaehler, A. Learning OpenCV: Computer Vision with the OpenCV Library. O'Reilly Media, Sebastopol, CA (2008).